IEEE Access
Multidisciplinary | Rapid Review | Open Access Journal

Received May 1, 2022, accepted May 26, 2022, date of publication June 6, 2022, date of current version June 10, 2022.

Digital Object Identifier 10.1109/ACCESS.2022.3180501

Second-Order Rotating Sliding Mode Control With Composite Reaching Law for Two Level Single Phase Voltage Source Inverters

FAHEEM HAROON[1], MUHAMMAD AAMIR[2], AND ASAD WAQAR[1]
[1]Department of Electrical Engineering, Bahria School of Engineering & Applied Sciences Islamabad Campus (BSEAS-IC), Islamabad 44000, Pakistan
[2]Pak-Austria Fachhochschule: Institute of Applied Sciences and Technology, Haripur 22620, Pakistan

Corresponding author: Faheem Haroon (faheemharoon.buic@bahria.edu.pk)

This work was supported technically in part by Bahria University, Islamabad, Pakistan; and supported technically in part by the Pak-Austria Fachhochschule: Institute of Applied Sciences and Technology, Haripur, Pakistan, through Higher Education Commision (HEC) Pakistan National Research Program for Universities in University, Science, Pakistan (NRPU) Grant: 20-17507/NRPU/R&D/HEC/2021.

ABSTRACT In the recent past, the integration of distributed generation via power electronic interface like voltage source inverter (VSI) allows attaining the desired voltage quality by adopting appropriate control law. This paper presents sliding mode control (SMC) with composite reaching law technique for regulating output voltage under variable load conditions for single phase VSI. Inherent properties of SMC like robustness are achieved usually at the cost of chattering along the sliding surface. To handle this trade-off, optimal sliding surface selection mechanism is applied with adoptive reaching law based on state variables magnitude to set the value of control gain. The novelty of the proposed technique is related to composite reaching law that overcomes constraints associated with SMC. The proposed reaching law is a combination of exponential, power, and difference function. The intelligent mix of these functions makes the suggested reaching law more effective in achieving a high-speed convergence rate of system states and significant chattering reduction. Moreover, the sliding surface is chosen using a time-varying slope based on error variables. Comparative study of SMC with cosine exponential reaching law (Cos-ERL) results, fractional power rate reaching law (FPRRL) and proposed composite reaching law with rotating sliding surface(C-RL-RSS) applied on single phase voltage source inverter under variable load conditions validates the effectiveness of the proposed C-RL-RSS based SMC. It is revealed that the proposed C-RL-RSS based SMC is proficient in achieving very low %THD in the output voltage along with reduced chattering and minimum tracking time.

INDEX TERMS Sliding mode control, single phase voltage source inverter, reaching law, sliding surface.

I. INTRODUCTION

Voltage source inverter (VSI) is the most momentous dc-ac element of several advanced applications. That covers the wide range of utilization starting from tiny car adapters, household, and industrial applications to the large grid-systems. Very frequent advancements in science and technology, aerospace, communication, defense sector, hospitals, and power storage equipment require a high quality power supply. Moreover, unexpected interruptions and outages may lead to data storage loss, program destruction, or even malfunctioning electronic equipment. Therefore, a well-regulated, clean and continuous power supply is of great importance.

The associate editor coordinating the review of this manuscript and approving it for publication was Chandan Kumar.

Single phase voltage source inverters (SPVSI) are meant to supply well-regulated ac voltage with low %THD and frequency in stand-alone mode of operation. Moreover, 33stand-alone SPVSIs have to provide suitable disturbance rejection mechanisms with fast transient and dynamic responses for sudden load variations [1], [2]. According to European Standard EN 62040-3 [3], uninterrupted power supply (UPS) is divided into three categories depending upon their application and structure i-e. on-line, off-line, and line-interactive UPS. Off-line UPS is one of the applications of stand-alone SPVSI, adopted in every walk of life. The principal purpose of UPS is to ensure power supply to critical loads when the utility fails to supply power. All these applications and sensitivity associated with the reliable and safe performance of SPVSI call for exceptionally reliable control and an effective response mechanism to handle any credible contingency.

Therefore, a control for SPVSI must be designed to fulfill multiple objectives. First of all, the controller must guarantee flawless reference tracking with good disturbance rejection capability. That leads to well-regulated output voltage with minimum total harmonic distortion %THD under linear and non-linear loads. Secondly, good dynamic response during load varying conditions is highly desired [4]. It is a common observation that under the condition of heavy load for SPVSI, the transient response of the controller is severely affected [5]. Thus, the controller for VSI must be capable of achieving the abovementioned objectives during unexpected output load variations.

Nowadays, voltage source inverter-based systems are working very near to stability constraints in order to cater financial and environmental concerns. However, ensuring a stable, reliable, and effective voltage source inverter's output for sensitive systems is still a challenging task. Thus, a control system for SPVSI must be designed to achieve the aforementioned objectives. Sliding mode control is a non-linear controller derived from the continuous-time variable structure control theory and was introduced initially in 1950 in Russia by Emelyanov and several other co-researchers [6], [7]. SMC has some inherent properties like simple design, reduced order, and exceptional robustness. Moreover, SMC is insensitive to external disturbances and parametric variations, finite-time convergence, and excellent dynamic behavior. Due to exponential robustness, SMC has been studied extensively for the first time in the theoretical research domain [8] and later on applied to industrial applications [9]. Due to its inherent characteristics, SMC is a widely adopted technique in several non-linear systems, including voltage source inverter applications. In SMC, the sliding surface is selected such that states of the system are compelled to reach the sliding surface in a limited time. With this, system dynamics become linear time-varying stable, having negligible internal or external disturbances. Irrespective of asymptotic convergence of states to the sliding surface, conventional SMC, like other non-linear control techniques, suffer from many imperfections.

In this perspective, two major areas need utmost attention. First, the first major shortcoming that SMC suffers is related to a fixed sliding surface that restricts the dynamic behavior of the feedback system. The fixed value of the sliding surface slope is a compromise between tracking time under output current disturbances and the reaching time of the system states to the sliding surface [10]. To achieve faster response, adjustable sliding surface techniques were proposed [11], [12]. 2-D and 1-D fuzzy-based rules were adopted in [13] and [14], respectively. In [15], rotation of sliding surface is obtained as a linear function of approximation from input-output relation based on 1-D Fuzzy rule. Moreover, extension to this mechanism is applied to a single-input fuzzy logic controller (SIFLC) based on error variables to adjust the time-varying slope of sliding surface, that leads to rotating sliding surface (RSS) to achieve fast transient response for single phase voltage source inverters [10]. With all the advantages and simplicity for designing sliding surfaces, the abovementioned techniques are a linear approximation for non-linear state space variables. Also, only surface rotation mechanism is adopted, overlooking the significance of switching gain of reaching law.

The second vital issue is that SMC often uses the high value of switching gains to achieve robustness. However, the choice of high gains can lead to severe problems related to chattering [16]. Using saturation function instead of switching function can be a favorable choice to overcome chattering. Although, chattering catered through this choice still results in a steady-state error due to boundary layer choice. Gudey and Gupta *et al.* [17] proposed recursive fast terminal sliding mode control for SPVSI with a condition to avoid singularity, which leads to shortening tracking and sliding time with a merely noticeable reduction in tracking error. Moreover, tuning constants to avoid singularity conditions and sliding coefficients for sliding surfaces designs are selected randomly. The effect of the RFT-SMC on the chattering problem on the sliding surface is also ignored in the analysis. Numerous strategies have been adopted to overcome the aforementioned problem, like second-order sliding mode control (SoSMC) [18], [19]. The primary purpose of using SoSMC is to eliminate chattering by allowing the switching function and its derivatives to converge to equilibrium point through integral function. To improve the performance of SoSMC, efforts were made using the super twisting control technique [20], [21]. Later on, actions like modified super twisting algorithms were integrated with SoSMC to achieve better performance [22], [23]. With all these benefits, there is higher chances of system instability due to a second-time derivative of switching surface that multiplies the risk to external disturbances.

To overcome aforementioned problems, worth mentioning innovative techniques have been proposed, like higher-order sliding mode control (HoSMC) [24], [36]–[38], complementary sliding mode control [25], and the most popular reaching law technique (RL) [26]. HoSMC is preferred to use in higher order multiple input multiple output (MIMO) systems [39]. Since SPVSI is a second order single input single output(SISO) system, therefore due to high level of complexities associated with implementation of HoSMC [40], it is not preferred to use in second order systems like SPVSI.

The reaching law technique directly correlates with the convergence rate of system states to the equilibrium point. Therefore, reaching time of SMC along with chattering reduction can be achieved through intelligent design of a reaching law. Gao *et al.* [27] proposed a switching function associated with variable structure control and reaching laws such as constant reaching law, proportional reaching law, and power reaching law. However, sliding surface design is also one of the essential parameters in designing SMC SPVSI systems. Generally, a sliding surface function is a linear combination of error and its derivative.

Several techniques have been proposed in the literature to minimize reaching time while taking care of chattering on the sliding surface. Fixed gain reaching law enforces system states to converge on sliding surface ($S = 0$) infinite reaching time [28]. The time required to converge the surface depends on the value of the control gain value. Thus, a higher value of gain ensures faster convergence while giving rise to chattering along the sliding surface. Fixed with proportional gain reaching law employs faster convergence, however lack in mitigation of chattering along the surface. A breakthrough in tackling the issue occurs with the advent of power gain reaching law [29], in which reaching time speed is adjustable with the distance of states from the sliding surface. Hence, ensuring fast convergence with reduction of chattering. However, very near the surface, the value of gain is not eliminated, thus causing chattering. Through analysis of three reaching gain laws, it can be easily deduced that these laws are beneficial in achieving better results through simple designing of sliding mode control. However, each control gain reaching law has its merits and minor demerits, which always leads to a compromise between reaching speed and chattering mitigation or control robustness and chattering reduction. The commonality among these laws is that convergence time to reach the desired sliding surface is directly dependent upon the value of reaching law gain. The higher value of gain always leads to chattering along the surface that has higher frequency dynamics.

To handle this compromise better, exponential reaching law (ERL) was introduced [30]. That, proves efficient in handling trade-offs between reaching time, chattering, and robustness of control. Interestingly, the E-RL has catered the trade-off by allowing the controller to adjust the gain value according to the surface variation. The idea has been widely accepted and adopted since then and applied to robust control in several non-linear systems of various fields.

In [31], [32], along with achieving robustness and reduced overshoot, chattering along the sliding surface is also reduced through applying slight changes to exponential reaching law. A modified E-RL proposed in [31] results in reduced chattering and lower total harmonic distortion value. Discrete-time repetitive sliding mode control based on E-RL with bi-power characteristics applied to three-phase voltage source inverters to achieve better steady-state response with robustness [32]. In [33], using the cos function with exponential and power term (Cos-ERL) further improves the reaching time with a noticeable reduction in chattering across the surface. However, a lower bound of the control gain is maintained at $Lsign(S)$, limiting the convergence behavior of a reaching law. It's observed that the system's state variables do not follow the system trajectory perfectly following the lower value of chattering.

Hence, multiple limitations found in existing reaching laws, a few of which are listed below, gives enough motivation to devise a mechanism to further increase the convergence rate of system states to the equilibrium point with maximum chattering reduction:

i. Most scholarly work focuses single part of SMC at a time for a specific system of VSI, i-e. Sliding surface or a reaching law.
ii. The value of the sliding surface coefficient affects the dynamic performance of stand-alone SPVSI, i-e for a small value of the sliding coefficient. Time to track the reference voltage increases while reaching time lasts longer at a higher sliding coefficient value. Therefore, the selection of optimal sliding coefficients is essential for every SPVSI system.
iii. Inherent properties of robustness and simplicity make SMC the most favorable choice to be used in SPVSI systems. Reaching gain plays a pivotal role in achieving robustness, which can be fixed or set through reaching law. Robustness is achieved through a higher value of gain, resulting in increased chattering along the sliding surface, which is undesirable.
iv. Several effective techniques have been implemented to design reaching law to achieve robustness with reduced chattering along the surface. However, there is still necessary for SPVSI systems to further enhance robustness with reduced chattering.

Hence, the main contributions of this article can be summarized as:

i. A composite control gain reaching law function is proposed using exponential reaching law with cos function integrated with difference and power function. The smart integration of these functions results in achieving improved convergence rate to guarantee robustness without effecting chattering mitigation. The proposed law is very adaptive concerning the distance of system states from the sliding surface, i-e. At a longer distance, the magnitude of gain is higher to achieve robustness. While, as the distance decreases, the proposed law sets the smaller value of gain magnitude to avoid chattering along the sliding surface.
ii. SMC-based control is designed for stand-alone SPVSI with a rotating sliding coefficient selection method based on SIFLC and novel reaching law.
iii. Behavior of the proposed control is tested on a second order system to examine responses with a high and low value of gains. Moreover, Cos-ERL [33] based SMC and FPRRL [35] based control are also tested on the same system, and it is shown that at different values of gains, the proposed system behaves best in achieving fast convergence with reduced chattering.
iv. The proposed reaching law based SMC technique is applied on single phase VSI under variable non-linear load conditions to achieve extremely fast convergence with little chattering and reduced %THD. Furthermore, Cos-ERL [33] based SMC and FPRRL [35] based SMC

are also tested on single-phase VSI to prove the validity of the proposed reaching law based SMC.

II. PROPOSED COMPOSITE EXPONENTIAL REACHING LAW

In [35], the theory of SMC for non-linear systems is well-explained. The general equation for a dynamic non-linear second order system is given below:

$$\ddot{x} = f(x, \dot{x}) + b(x, \dot{x})\, u \tag{1}$$

where $f \in \Re^n$ and $b \in \Re^{nXn}$ are non-linear functions, u is the control input and b is an invertible matrix. The tracking output error that ultimately goes to zero can be defined as $\tilde{x}(t) = x - x_d$, where $x_d \in \Re^n$ is the desired output. The first step to design SMC is always to start selecting appropriate switching function S that depend on tracking error. Generally, the sliding surface equation is described as:

$$S = \dot{\tilde{x}} + \lambda_s \tilde{x};\ \lambda_s > 0 \tag{2}$$

where λ_s is termed as the slope of sliding surface or sliding surface coefficient, the value of λ_s plays a very significant role in the convergence of tracking output error to zero.

A. STABILITY ANALYSIS

The well-known Lyapunov function can be described as $V(S) = \frac{1}{2} S^T S$; by taking derivative, we get the following equation:

$$\dot{V} = S^T \dot{S} \tag{3}$$

The stability condition is described as:

$$\dot{V} < 0 \Longrightarrow \begin{cases} \dot{S} < 0 & if\ S > 0 \\ \dot{S} > 0 & if\ S < 0 \end{cases}$$

Thus the control input for system (1) can be rearranged as:

$$u = b^{-1}[\ddot{x}_d - \lambda_s \dot{\tilde{x}} - f + \dot{S}] \tag{4}$$

The vital role of $\dot{S}$ in input control function can be observed easily, i-e the rate of change of sliding surface S is determined by $\dot{S}$. So, at $\dot{S} \ll 0$ for $S > 0$ (and vice versa) forces the system trajectories to reach and converge at $S = 0$.Thus, the term $\dot{S}$ is well-known as ''reaching law''. Moreover, when states of the system are very close to $S = 0$, $\dot{S} < 0$ determines that system states are near to $S = 0$ while guaranteeing $\dot{V} < 0$. Subsequently, there is a ''switching'' mechanism arises to maintain the condition: $S\dot{S} < 0$.

In this portion, the mathematical development of the proposed control gain reaching law is presented. The proposed control gain reaching law links the advantages mentioned in referenced reaching laws and guarantees a better convergence rate than previous ERL(s). The proposed Control Gain Reaching Law uses sinusoidal damping concept from [33] using exponential term tailored with difference function, and is stated as:

$$\dot{S} = \left[D(S) - \frac{G(|S|)}{E(S)} \right] sign(S)$$

$$D(S) = |S|\left(\gamma + (1-\gamma)\, e^{-\varphi |S|^{\$}}\right)$$
$$E(S) = \gamma + (1-\gamma)\, e^{-\varphi |S|^{\$}} \cos(\beta(|S|)) \tag{5}$$

where $0 < \gamma < 1, \varphi > 0, \$ > 0, \beta > 0$ *and* $G > 0$ The first derivative of sliding surface $\dot{S}$, defines the reaching law. To achieve stability, the Lyapunov function $V(t) = S^2/2$ must be minimum, following condition $\dot{V}(t) < 0$.The gain value of proposed reaching law $\left[D(S) - \frac{G(|S|)}{E(S)} \right]$ is strictly negative, warranting $S\dot{S} < 0$.

The working principle of the proposed control gain reaching law can be explained as follows:

i. Initially at $S \gg 0$, value of control gain reaching law will be maximum following initial control loop system conditions.
ii. Values of $\varphi, \$ and \beta$ are selected in such a way that for $e^{-\varphi |S|^{\$}} \cos(\beta(|S|) \approx 0 \Longrightarrow E(S) \approx \gamma \rightarrow E(S) < 1$ leads to a higher value of $\frac{G|S|}{E(S)}$ where $D(S) < \frac{G|S|}{E(S)}$ ensures gradual system convergence to $S = 0$.
iii. At $S \approx 0 \rightarrow E(S) \approx 1$ leads to $\frac{G|S|}{E(S)} < 1$, hence $D(S) < \frac{G|S|}{E(S)}$ leads to negligible control gain of reaching law i-e $\left[D(S) - \frac{G|S|}{E(S)} \right] sign(S) \rightarrow 0$ that ensures extremely low chattering along the sliding surface.

Control gain of the proposed reaching law is the most efficient convergence mechanism for system states to reach equilibrium point in finite time. The term $e^{-\varphi |S|^{\$}} \cos(\beta(|S|)$ has damping characteristics to cross surface several times and asymptotically coincide to the reference point [33]. Moreover, the difference function $D(S)$ has an added advantage to gain adjustment and ensures negligible control gain value at an equilibrium point.

Latest and state of the art reaching laws like ERL [32], Cos-ERL [33], enhanced exponential reaching law (EERL) [31], power rate exponential reaching law(PRERL) [34], fractional power rate reaching law (FPRRL) [35] and proposed C-ERL-RSS shown in Table-1 along with comparative analysis of their behavior with changing surface position from the equilibrium point is shown in Fig.1, which strongly advocates the proposed law's effective and adaptive characteristics.

It can be seen that when the surface is at $S = 2$ far away from $S = 0$ on the x-axis, at this point magnitude of control gain on the y-axis must be higher to ensure robustness. At the same time, it is clear from the graph of Fig.1 that the value of magnitude of gains for ERL, Cos-ERL, PRERL and EERL [31] are lesser than the value of gain of proposed C-ERL-RSS. Thus ensuring robustness of the proposed reaching law. Though, the value of gain of FPRRL at $S = 2$ is a bit higher than the proposed reaching law, thus achieving fast response at higher surface value. However, the FPRRL [35] fails to lower it's gain value at a higher pace towards the $S = 0$,thus causing extremely higher chattering. Moreover, as the surface moves to the left of the graph, towards the equilibrium point i-e $S = 0$, the value of the magnitude of gain shall be reduced respectively. However, from the graph it is evident that gain magnitude for ERL [32] and Cos-ERL [33]

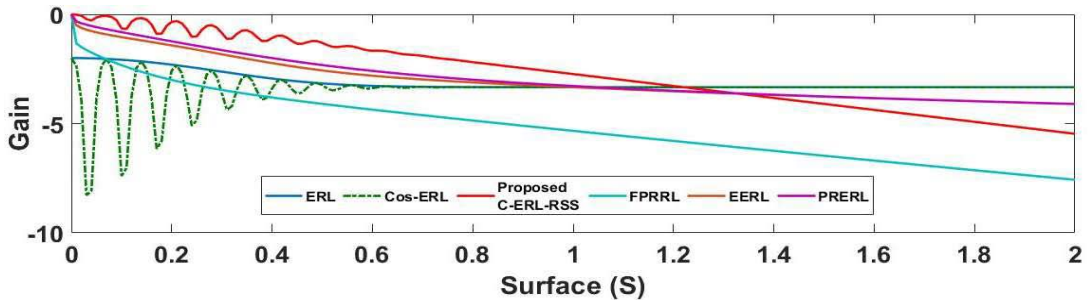

FIGURE 1. Comparison of reaching laws gain variation w.r.t distance from surface.

TABLE 1. Reaching laws with parametric values.

	Reaching Law	Parameters
ERL[32]	$\dot{S} = \left[-\frac{G}{(\gamma+(1-\gamma))e^{-\varphi\lvert S\rvert^{\pounds}}}\right] sign(S)$	$\gamma = 0.6, \varphi = 10,$ $G = 2, \pounds = 2$
Cos-ERL[33]	$\dot{S} = \left[-\frac{G}{(\gamma+(1-\gamma))e^{-\varphi\lvert S\rvert^{\pounds}}\cos(\beta(\lvert S\rvert))}\right] sign(S)$	$\gamma = 0.6, \varphi = 10, \pounds = 2,$ $\beta = 85, G = 2$
FPRRL[35]	$\dot{S} = \left[-\frac{G\lvert S\rvert^{\tau}}{\delta+\theta\lvert S\rvert}\right] sign(S)$	$G = 2, \tau = 0.3$ $\delta = 0.1, \theta = 0.01$
PRERL[34]	$\dot{S} = \left[-\frac{G\lvert S\rvert^{\tau}}{(\gamma+(1-\gamma))e^{-\varphi\lvert S\rvert^{\pounds}}}\right] sign(S)$	$G = 2, \tau = 0.3$ $\gamma = 0.6, \varphi = 10,$ $\pounds = 2$
EERL[31]	$\dot{S} = \left[-KS - \frac{G\lvert S\rvert}{(\gamma+(1-\gamma))e^{-\varphi\lvert S\rvert^{\pounds}}}\right] sign(S)$	$K = 200, G = 2$ $\gamma = 0.6, \varphi = 10,$ $\pounds = 2$
Proposed C-ERL-RSS	$\dot{S} = \left[\lvert S\rvert(\gamma+(1-\gamma))e^{-\varphi\lvert S\rvert^{\pounds}} - \frac{G\lvert S\rvert}{(\gamma+(1-\gamma))e^{-\varphi\lvert S\rvert^{\pounds}}\cos(\beta(\lvert S\rvert))}\right] sign(S)$	$\gamma = 0.6, \varphi = 10, \pounds = 2,$ $\beta = 85, G = 2$

TABLE 2. Comparison of reaching laws in terms of robustness and chattering.

Reaching Law	Robustness	Chattering
ERL	Low	High
Cos-ERL	Low	High
EERL	Moderate	Moderate
PRERL	Moderate	Moderate
FPRRL	High	High
Proposed C-ERL-RSS	High	Low

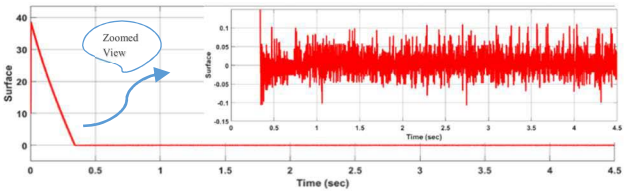

FIGURE 2. Tradeoff-tracking time vs chattering for Cos-ERL [33] with low value of gain.

is constant till $S = 0.7$, further to the left on the graph value of gain magnitude reduced to 2 at $S = 0$.This high level of gain magnitude at $S = 0$ results in high chattering. The behavior of EERL [31] and PRERL is improved in comparison to ERL [32] and Cos-ERL [33] in terms of chattering reduction and fast response. However, in the case of the proposed C-ERL-RSS, the value of gain magnitude at $S = 2$ is higher that ERL [32], Cos-ERL [33], EERL [31], PRERL [34], thus ensuring robustness. The value of gain for proposed C-ERL-RSS near to the equilibrium point $S = 0$ is less that all the other reaching laws,thus ensuring extreme chattering reduction. Therefore, the proposed C-ERL-RSS can achieve high robustness with extremely reduced chattering along the sliding surface, $S = 0$.

The reaching law proposed in this paper and reaching law proposed in [33] and [35] are tested on a second-order system described in (1) with the same values of parameters shown in Table-I to examine and analyze the trade-off between tracking time and chattering along the sliding surface at high and low values of gain. The tracking time and chattering response of reaching law proposed in [33] are shown in Fig.2 and Fig.3 at low and high gain values, respectively. It can be observed from Fig.2 that at a low gain value of 50, the tracking time is 0.36sec with a chattering of 0.2v. However, in Fig.3, at a high gain value of 5000, the tracking time is extremely reduced to 0.045sec with a high rise in the chattering of 1.62v, which is very undesirable. On the other hand if we observe the behavior of FPRRL [35] under low and high gain shown in Fig.4 and Fig.5, respectively. It can be observed that the chattering is considerably reduced in Fig.4, while the overshoot of 0.35v occurs which leads to high reaching time of 0.45sec. Moreover, there is a steady state error along the surface and zero crossing doesn't take place after 0.45sec. Moreover, if we observe behavior under high gain value, the noticeable increase in chattering takes place and overshoot still occurs that leads to just improved tracking time of 0.2sec. The chattering with overshoot and steady state error with low value of gain is undesirable.

However, the response of reaching law proposed in this paper (C-ERL-RSS) is shown in Fig.6 and Fig.7 at low and high gain values, respectively. In Fig.6 tracking time of 0.4sec is achieved with a chattering of 0.05v at a low gain value of 50. While at a high gain value of 5000, tremendous

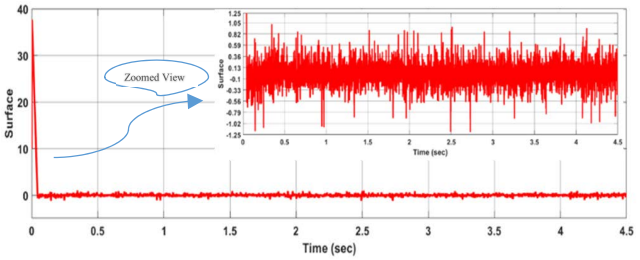

FIGURE 3. Tradeoff-tracking time vs chattering for Cos-ERL with high value of gain.

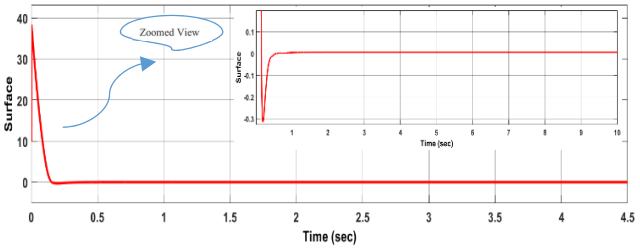

FIGURE 4. Tradeoff-tracking time vs chattering for FPRRL with low value of gain.

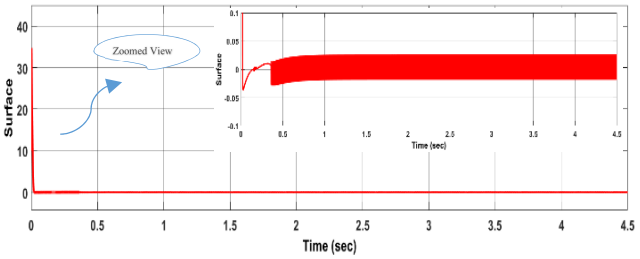

FIGURE 5. Tradeoff-tracking time vs chattering for FPRRL with high value of gain.

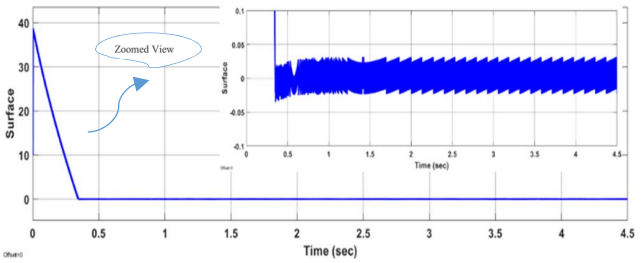

FIGURE 6. Trade-off – tracking time & chattering for proposed C-ERL-RSS with low value of gain.

improvement in tracking time can be observed i-e. tracking time is reduced to 0.31sec. At the same time, a slight increase in the chattering of 0.45v is observed. The proposed C-ERL-RSS has shown 400% better robustness with 2.34% less chattering than the Cos-ERL reaching law [33]. Thus, the proposed reaching law has proven its capability of assuring robustness with minimum chattering along the sliding surface.

TABLE 3. Comparison of proposed C-ERL-RSS with COS-ERL [33] and FPRRL [35].

Reaching Law	Cos-ERL [33]		FPRRL[35]		Proposed C-ERL-RSS	
Gain=50	0.36sec	0.2v	0.45sec	0.001v	0.4sec	0.05v
Gain=5000	0.045sec	1.62v	0.2sec	0.05v	0.031sec	0.5v
Effect	800% Reduced	12.34% Increased	225% Reduced	50% Increased	1212% Reduced	10% Increased
Parameter	Tracking Time	Chattering	Tracking Time	Chattering	Tracking Time	Chattering

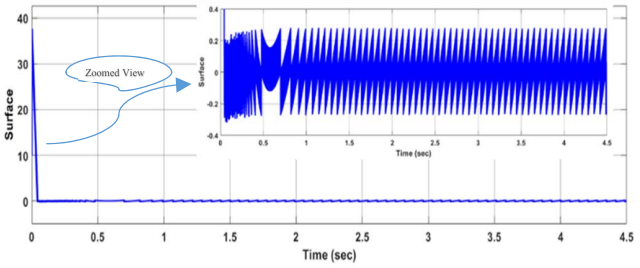

FIGURE 7. Trade-off – tracking time & chattering for proposed C-ERL-RSS with high value of gain.

III. SYSTEM MODELING FOR SINGLE PHASE VSI

The single-phase voltage source inverter is shown in Fig.8.The following state space equations can describe the operation of the system:

$$\frac{d}{dt}\begin{bmatrix} v_0 \\ i_L \end{bmatrix} = \begin{bmatrix} 0 & 1/C \\ -1/L & 0 \end{bmatrix}\begin{bmatrix} v_0 \\ i_L \end{bmatrix} + \begin{bmatrix} 0 \\ V_S/L \end{bmatrix} u + \begin{bmatrix} -i_0/C \\ 0 \end{bmatrix} \tag{6}$$

where u is the control input.

The output voltage error and its derivatives can be defined as

$$x_1 = v_0 - v_0^* \tag{7}$$

$$x_2 = \dot{x}_1 = \dot{v}_0 - \dot{v}_0^* = (i_C - i_C^*)/C \tag{8}$$

where v_0^* is the derivative of a reference voltage selected as $v_0^* = V_m \sin(\omega t)$

System behavior can be described in the following state space form:

$$\begin{bmatrix} \dot{x}_1 \\ \dot{x}_2 \end{bmatrix} = \begin{bmatrix} 0 & 1 \\ -1/LC & 0 \end{bmatrix}\begin{bmatrix} x_1 \\ x_2 \end{bmatrix} + \begin{bmatrix} 0 \\ V_S/LC \end{bmatrix} u + \begin{bmatrix} 0 \\ \mathbf{D}(t) \end{bmatrix} \tag{9}$$

where disturbance term $D(t)$ is given as:

$$D(t) = \begin{bmatrix} 0 \\ -\left(\frac{1}{C}\right)\frac{di_0}{dt} - \left(\frac{1}{LC}\right)v_0^* - \frac{d\dot{v}_0^*}{dt} \end{bmatrix}$$

It is worth noting that due to the derivative of load current, $D(t)$ is not bounded.

IV. SMC WITH PROPOSED REACHING LAW

The sliding surface equation for a given system is given as:

$$S = \lambda x_1 + x_2 \tag{10}$$

where,

$$x_2(t) = \dot{x_1}(t) \tag{11}$$

Substituting eq(7) and eq(8) in eq(10)

$$S = \lambda \left(v_0 - v_0^*\right) + \left(\frac{i_C}{C} - \dot{v_0^*}\right) \tag{12}$$

$$\dot{S} = \lambda \dot{x_1}(t) + \ddot{x_1}(t) \tag{13}$$

Substituting eq(5) in eq(13)

$$\left[|S|\left(\gamma + (1-\gamma)\right) e^{-\varphi|S|^{\$}} - \frac{G\,|S|}{\left(\gamma + (1-\gamma)\right) e^{-\varphi|S|^{\$}} \cos\left(\beta\left(|S|\right)\right)}\right] sign\,(S) = \lambda \dot{x_1}(t) + \ddot{x_1}(t) \tag{14}$$

where $0 < \gamma < 1, \varphi > 0, \$ > 0, \beta > 0, \lambda > 0$ *and* $G > 0$ $\ddot{x}_1\,(t) = \dot{x_2}$, there from a control function in (9) with proposed reaching, law Can be described as (15) and (16), as shown at the bottom of the next page. In order to achieve rotating sliding surface (RSS), the value of sliding surface coefficient λ is set by using time-varying slope of a sliding surface. Thus, different values of λ can be achieved during transient and steady-state operations. It is shown in [10] that sliding surface with time-varying slope λ can be rotated in phase plane under load varying conditions. It is worth mentioning here that SPVSI operates with a greater value of λ during a transient caused by load variation to achieve faster voltage convergence. However, the value of λ returned back to its original value and remains unchanged during steady-state. This dynamic characteristic of time-varying slope can be achieved simply by adopting a function of first order using error variables of the system. Thus, the function based on single-input fuzzy logic controller (SIFLC) rules using error magnitude applied in [44] shown below is used to achieve RSS:

$$\lambda = -0.45X_d + 0.5 \tag{17}$$

where,

$$X_d\,(t) = |X_1(t)| - \left|\dot{X}_2(t)\right| \tag{18}$$

The parametric values used in all three SMC controllers with Cos-ERL [33] based SMC, FPRRL [35] based SMC & proposed C-ERL-RSS based SMC, are chosen through intelligent guess using hit and trial method, shown in Table-4. It is worth mentioning that the exact value of all the common parameters between proposed C-ERL-RSS, FPRRL [35] and Cos-ERL [33] are used on SPVSI under the same conditions.

V. SIMULATION STUDY

In this portion of the paper, trajectory tracking of Cos-ERL [33], FPRRL [35] and proposed C-ERL-RSS implemented in Matlab/Simulink software for single SPVSI under variable load conditions are shown. A non-linear diode rectifier load of 1kW is applied at 0.045sec to test the behavior of proposed control scheme along with Cos-ERL and FPRRL under sudden load variations. The control parameters and circuit specifications are shown in Table-4 and Table-5, respectively. One can easily analyze that the SPVSI with proposed C-ERL-RSS shows fast convergence with robust trajectory tracking, shown in Fig.13. However, response of SPVSI with Cos-ERL and FPRRL, shown in Fig.11 and Fig.12 respectively, lacks in tracking the required trajectory.

The reference tracking characteristics of output voltage for Cos-ERL [33] based SMC, FPRRL [35] based SMC and proposed C-ERL-RSS based SMC are shown in Fig.14, Fig.15 and Fig.16, respectively.

TABLE 4. Parameters of controllers.

Gains	Cos-ERL SMC[33]	FPRRL[35]	C-ERL-RSS SMC Proposed
γ	0.6		0.6
φ	10	-	10
£	02	-	02
G	500	500	500
τ	-	0.3	-
δ	-	0.1	-
θ	-	0.01	-
β	85	-	85

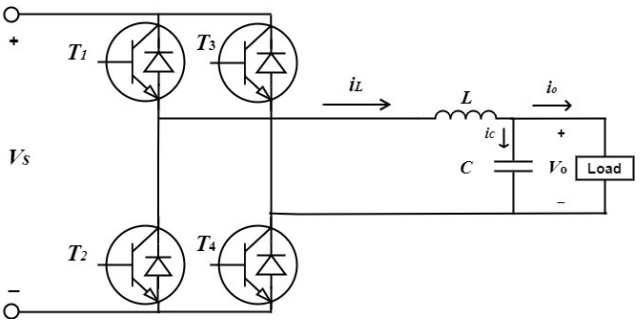

FIGURE 8. Single phase voltage source inverter(SPVSI).

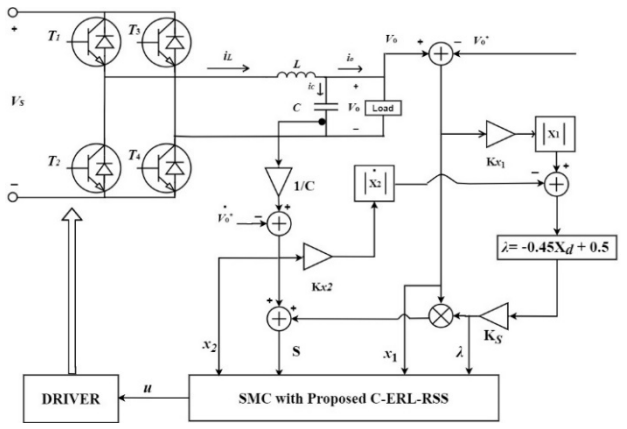

FIGURE 9. Block diagram of single phase voltage source inverter with proposed C-ERL-RSS.

TABLE 5. Circuit specifications.

Circuit parameter	Value
Input Source DC Voltage, V_s	300V
Reference peak voltage, V_m	200V
Filter Inductor, L	5.4Mh
Filter Capacitor, C	$46Uf$
Scaling Gain, K_{x1}	2×10^{-3}
Scaling Gain, K_{x2}	2.4×10^{-5}
Scaling Gain, K_S	30×10^{4}
Non-Linear rectifier Load	1KW
Switching Frequency[44]	21.67kHz

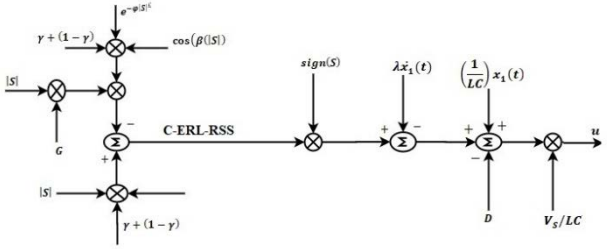

FIGURE 10. SMC with proposed C-ERL-RSS.

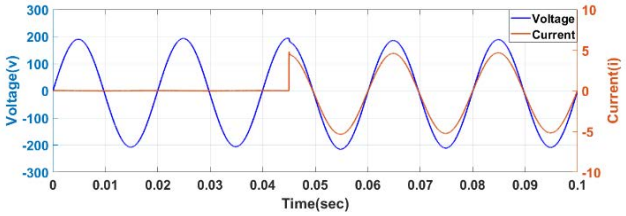

FIGURE 11. SPVSI output voltage and non-linear load current with Cos-ERL[33].

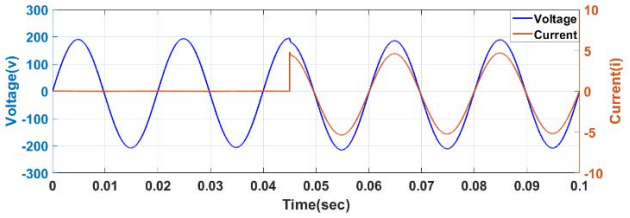

FIGURE 12. SPVSI output voltage and non-linear load current with FPRRL.

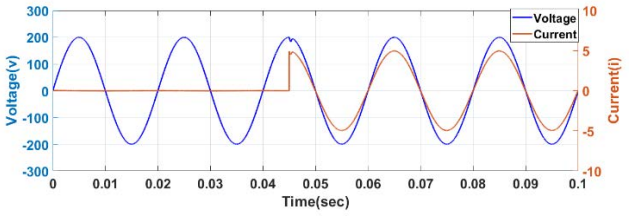

FIGURE 13. SPVSI output voltage and non-linear load current with proposed C-ERL-RSS.

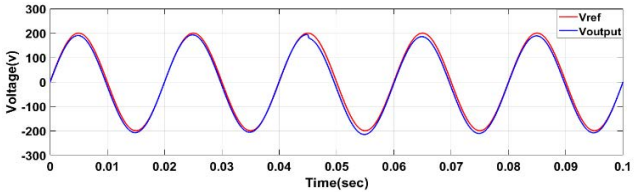

FIGURE 14. Voltage output reference tracking with Cos-ERL based SMC.

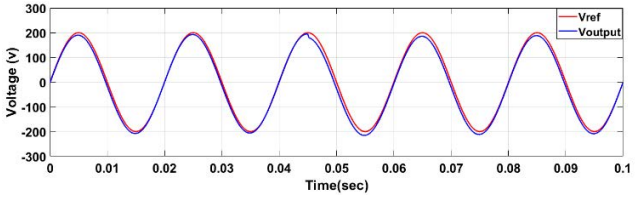

FIGURE 15. Voltage output reference tracking with FPRRL based SMC.

The reference tracking of the proposed C-ERL-RSS based SMC shown in Fig.16 shows the best tracking characteristics as the output voltage starts to follow the reference voltage in no time and stays on the reference trajectory hereafter. While Cos-ERL [33] based SMC and FPRRL [35] based SMC have very similar response in tracking the reference signal, that lacks in following the trajectory of required output voltage. Moreover, tracking is compromised after every half cycle.

To test the proposed C-ERL-RSS-based SMC behavior under load varying conditions, a non-linear diode rectifier load of 1kW is applied at 0.045sec. The output voltage response of Cos-ERL [33] based SMC, FPRRL [35] based

$$\left[|S|\left(\gamma+(1-\gamma)\right)e^{-\varphi|S|^{\$}}-\frac{G\,|S|}{\left(\gamma+(1-\gamma)\right)e^{-\varphi|S|^{\$}}\cos\left(\beta\left(|S|\right)\right)}\right]sign\left(S\right)$$
$$=\lambda\dot{x_1}\left(t\right)-\left(\frac{1}{LC}\right)x_1\left(t\right)+\left(V_S/LC\right)u \tag{15}$$

$$u(t)=LC/V_S\left[\begin{array}{l}\left[\left(|S|\left(\gamma+(1-\gamma)\right)e^{-\varphi|S|^{\$}}-\frac{G|S|}{\left(\gamma+(1-\gamma)\right)e^{-\varphi|S|^{\$}}\cos(\beta(|S|))}\right]sign\left(S\right)\\-\lambda\dot{x_1}\left(t\right)+(1/LC)x_1(t)-D\end{array}\right] \tag{16}$$

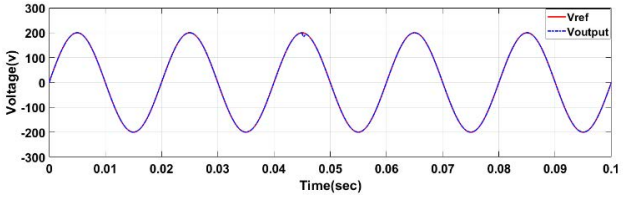

FIGURE 16. Voltage output reference tracking with proposed C-ERL-RSS based SMC.

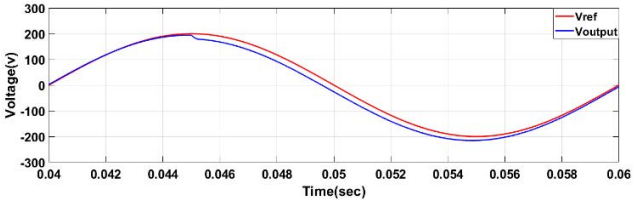

FIGURE 17. Output voltage waveform –Tracking Evolution under load variation with Cos-ERL [?] based SMC.

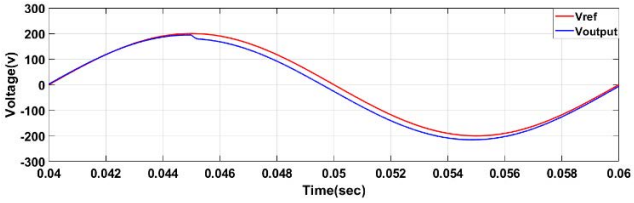

FIGURE 18. Output voltage waveform –tracking evolution under load variation with FPRRL based SMC.

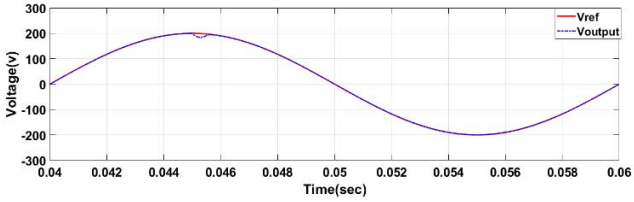

FIGURE 19. Output voltage waveform-tracking evolution under load variation with C-ERL-RSS based SMC.

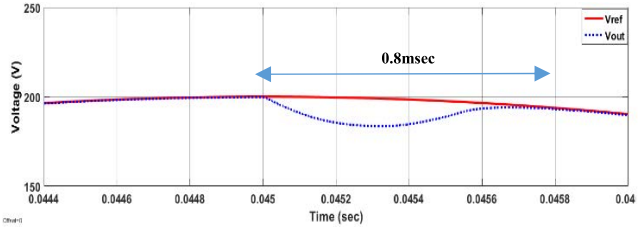

FIGURE 20. Zoomed view of step change response of non-linear load at 0.045sec.

SMC and C-ERL-RSS-based SMC under load varying conditions is shown in Fig.17, Fig.18 and Fig.19, respectively.

It can be observed from Fig.17 and Fig.18 that the output voltage takes 15msec to reach the reference trajectory. However, the output voltage only takes 0.8msec to reach the reference trajectory and follow the reference voltage

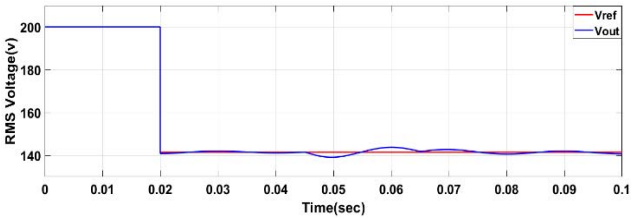

FIGURE 21. Steady-state response – Cos-ERL-SMC [?].

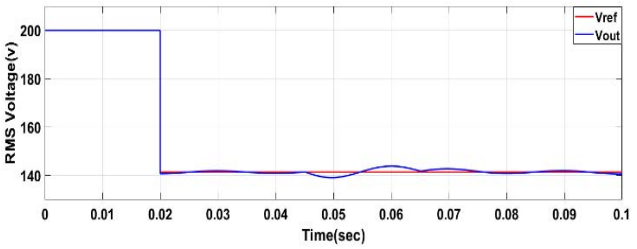

FIGURE 22. Steady-state response – FPRRL-SMC.

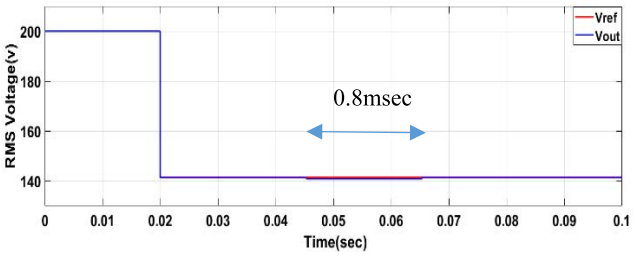

FIGURE 23. Steady state response – proposed C-ERL-RSS- SMC.

afterward, as shown in Fig.19. the response of the proposed C-ERL-RSS based SMC under varying load conditions is robust and spontaneous.

Moreover, steady state response for three techniques, Cos-ERL-based SMC, FPRRL based SMC and proposed C-ERL-RESS-based SMC, are shown in Fig.21, Fig.22 and Fig.23, respectively. Steady-state response shown in Fig.21 and Fig.22 is much slower. Also, under non-linear load applied at 0.045sec, much output deviation from the reference voltage can be seen in Fig.21 and Fig.22. While, the response of the proposed reaching law shown in Fig.23 is promising in achieving fast transient response with excellent behavior under load varying condition, as output attain its steady state just after 0.8msec with negligible output variation from the reference voltage.

Table-6 shows a comprehensive analysis of four reaching law based SMC(s) for SPVSI with diode rectifier non-linear load. The %THD obtained through the proposed technique is much smaller as compared to the other reaching law techniques. In addition, under load variation, output voltage starts tracking the reference voltage without any delay. A perfect balance of tracking time and chattering along the sliding surface is attained i-e tracking time along with chattering is considerably reduced even at a higher value of control gain.

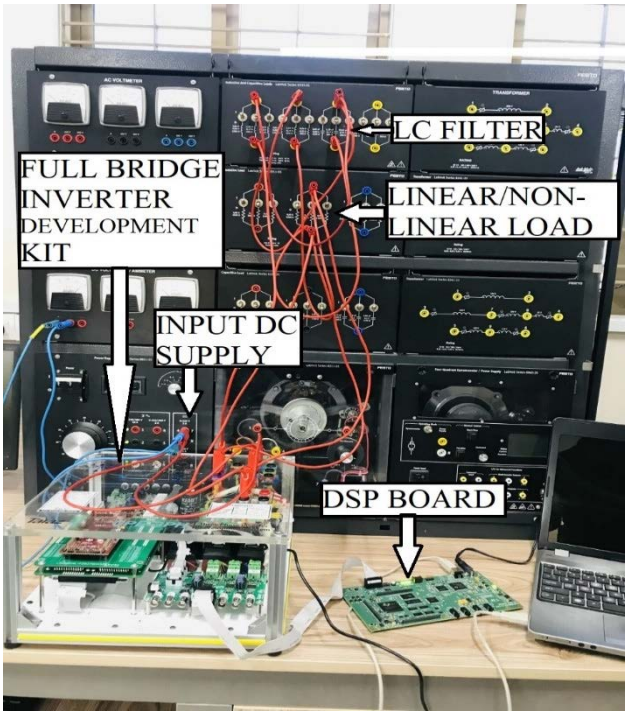

FIGURE 24. Experimental setup.

TABLE 6. Comparison of proposed C-ERL-RSS SMC with Cos-ERL [33], FPRRL [35] and RSS [10] SMC.

Category	RSS - SMC [10]	Cos-ERL SMC [33]	FPRRL SMC [35]	Proposed C-ERL-RSS SMC
THD(%)	2.66%	0.59%	0.61%	0.25%
Fundamental Voltage	196.7V	198.9V	198.3V	199.8V
Tracking Time	Low	Low	Low	Very Low
Chattering	Low	Low	Low	Very Low
Robustness	Good	Good	Good	Best
Steady-State Response	Good	Good	Good	Best

Thus, gaining maximum advantage from inherent properties of SMC like robustness. Adding to this, the proposed approach leads to a minor steady-state error in the output voltage.

VI. EXPERIMENTAL RESULTS

To demonstrate the competency and authenticity of proposed C-ERL- RSS based SMC for SPVSI system, a proposed control strategy is implemented through a Full Bridge Inverter Development Kit (SPM-FB-KIT) integrated with DSP board (TMS320C6713 DSK), DC input voltage of $V_s = 400V$, $V_m = 300V$, filter inductor $L = 250\mu H$, and capacitor $C = 100\mu F$, shown in Fig.9. Value of K_S is selected as 30×10^4 and values of other scaling gains K_{x1} and K_{x2} are selected as 2.4×10^{-5} and 30×10^4, respectively. The experimental behavior of proposed technique is tested under

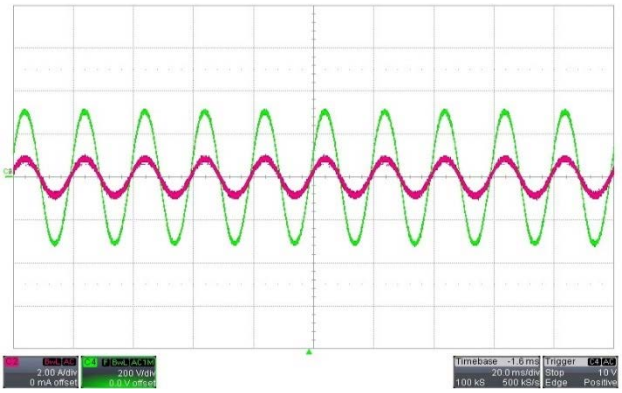

FIGURE 25. Experimental waveforms of output voltage (Green) 200V/div and current (Red) 2A/div under linear load.

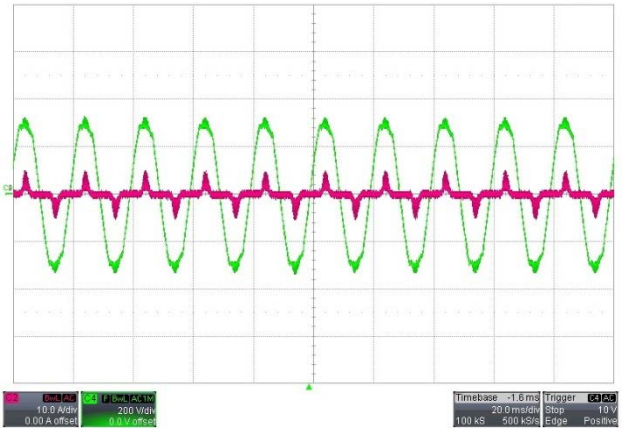

FIGURE 26. Experimental waveforms of output voltage(Green) 200V/div and current (Red) 10A/div under non-linear load.

linear and non-linear load. The response of output voltage and current under linear and non-linear load is shown in Fig.25 and Fig.26, respectively. Fig.25 testifies the capability of proposed C-ERL-RSS based SMC to achieve required output voltage profile along with stable load current and %THD of 0.69%. Moreover, output voltage achieved under non-linear load condition shown in Fig.26 affirms the effectiveness of proposed C-ERL-RSS based SMC to achieve required output voltage with % THD of 1.12%.

VII. CONCLUSION

A novel-reaching law based SMC for SPVSIs to fullfill the needs of susceptible systems is introduced. With proposed reaching law based SMC, the system becomes more reliable and capable of achieving robustness when subjected to load variations. It is shown that value of reaching law gain is intelligently adjusted to achieve fast tracking with little chattering even near the equilibrium point. The central concept of the proposed idea is to set the value of gain based on the distance of state variable from the sliding surface i-e gain value decreases with decreasing distance and vice versa. The effectiveness of the proposed reaching law is achieved through wise integration of exponential function, power function,

and difference function. Moreover, to achieve optimal surface, a rotating sliding surface selection mechanism is applied. The principle is based on linear approximation from the input and output relationship of SIFLC, working on the error magnitude of the system. The results achieved through the proposed reaching law advocate that lower THD (%) is achieved with an improved dynamic response.

ACKNOWLEDGMENT

The authors acknowledge the contributions and technical support of Bahria University, Islamabad, Pakistan, and Pak-Austria Fachhochschule: Institute of Applied Sciences and Technology, Haripur, Pakistan, under HEC's NRPU.

REFERENCES

[1] A. I. M. Ali, M. A. Sayed, and T. Takeshita, "Isolated single-phase single-stage DC-AC cascaded transformer-based multilevel inverter for stand-alone and grid-tied applications," *Int. J. Electr. Power Energy Syst.*, vol. 125, Feb. 2021, Art. no. 106534.

[2] L. Callegaro, C. Rojas, M. Ciobotaru, and J. Fletcher, "A controller improving photovoltaic voltage regulation in the single-stage single-phase inverter," *IEEE Trans. Power Electron.*, vol. 37, no. 1, pp. 354–363, Jan. 2022.

[3] (2018). *European Standard EN 62040-3*. [Online]. Available: https://files.stroyinf.ru/Data/704/70439.pdf

[4] I. Colak, E. Kabalci, and R. Bayindir, "Review of multilevel voltage source inverter topologies and control schemes," *Energy Convers. Manage.*, vol. 52, no. 2, pp. 1114–1128, Feb. 2011.

[5] Y. Wu and Y. Ye, "Internal model-based disturbance observer with application to CVCF PWM inverter," *IEEE Trans. Ind. Electron.*, vol. 65, no. 7, pp. 5743–5753, Jul. 2018.

[6] S. V. Emelyanov, *Variable Structure Control Systems*. Moscow, Russia: Nauka, 1967.

[7] V. Utkin, "Variable structure systems with sliding modes," *IEEE Trans. Autom. Control*, vol. AC-22, no. 2, pp. 212–222, Apr. 1977.

[8] B. Draženović, "The invariance conditions in variable structure systems," *Automatica*, vol. 5, no. 3, pp. 287–295, 1969.

[9] J. Y. Hung, W. Gao, and J. C. Hung, "Variable structure control: A survey," *IEEE Trans. Ind. Electron.*, vol. 40, no. 1, pp. 2–22, Feb. 1993.

[10] H. Komurcugil, "Rotating-sliding-line-based sliding-mode control for single-phase UPS inverters," *IEEE Trans. Ind. Electron.*, vol. 59, no. 10, pp. 3719–3726, Oct. 2012.

[11] S.-B. Choi, D.-W. Park, and S. Jayasuriya, "A time-varying sliding surface for fast and robust tracking control of second-order uncertain systems," *Automatica*, vol. 30, no. 5, pp. 899–904, May 1994.

[12] A. Bartoszewicz, "A comment on A time-varying sliding surface for fast and robust tracking control of second-order uncertain systems," *Automatica*, vol. 31, no. 12, pp. 1893–1895, Dec. 1995.

[13] S. Tokat, I. Eksin, and M. Guzelkaya, "New approaches for on-line tuning of the linear sliding surface slope in sliding mode controllers," *Turkish J. Elect. Eng.*, vol. 11, no. 1, pp. 45–59, 2003.

[14] F. Yorgancıoğlu and H. Kömürcügil, "Single-input fuzzy-like moving sliding surface approach to the sliding mode control," *Electr. Eng.*, vol. 90, no. 3, pp. 199–207, Feb. 2008.

[15] A. Šabanovic, "Variable structure systems with sliding modes in motion control—A survey," *IEEE Trans. Ind. Informat.*, vol. 7, no. 2, pp. 212–223, May 2011.

[16] F.-J. Lin, Y.-C. Hung, and M.-T. Tsai, "Fault-tolerant control for six-phase PMSM drive system via intelligent complementary sliding-mode control using TSKFNN-AMF," *IEEE Trans. Ind. Electron.*, vol. 60, no. 12, pp. 5747–5762, Dec. 2013.

[17] S. K. Gudey and R. Gupta, "Recursive fast terminal sliding mode control in voltage source inverter for a low-voltage microgrid system," *IET Gener., Transmiss. Distrib.*, vol. 10, no. 7, pp. 1536–1543, May 2016.

[18] Q. Tabart, I. Vechiu, A. Etxeberria, and S. Bacha, "Hybrid energy storage system microgrids integration for power quality improvement using four-leg three-level NPC inverter and second-order sliding mode control," *IEEE Trans. Ind. Electron.* vol. 65, no. 1, pp. 35–424, 2018.

[19] H. Wang, X. Ge, and Y. C. Liu, "Second-order sliding-mode MRAS observer-based sensorless vector control of linear induction motor drives for medium-low speed maglev applications," *IEEE Trans. Ind. Electron.*, vol. 65, no. 12, pp. 9938–9952, Mar. 2018.

[20] L. Derafa, A. Benallegue, and L. Fridman, "Super twisting control algorithm for the attitude tracking of a four rotors UAV," *J. Franklin Inst.*, vol. 349, no. 2, pp. 99–685, 2012.

[21] Y. Kali, M. Saad, K. Benjelloun, and C. Khairallah, "Super-twisting algorithm with time delay estimation for uncertain robot manipulators," *Nonlinear Dyn.*, vol. 93, no. 2, pp. 557–569, Jul. 2018.

[22] M. Defoort and M. Djemai, "A Lyapunov-based design of a modified super-twisting algorithm for the Heisenberg system," *IMA J. Math. Control Inf.*, vol. 30, no. 2, pp. 185–204, Jun. 2013.

[23] L. Fridman, J. Davila, and A. Levant, "High-order sliding-mode observation for linear systems with unknown inputs," *Nonlinear Anal., Hybrid Syst.*, vol. 5, no. 2, pp. 189–205, May 2011.

[24] F.-J. Lin, J.-C. Hwang, P.-H. Chou, and Y.-C. Hung, "FPGA-based intelligent-complementary sliding-mode control for PMLSM servo-drive system," *IEEE Trans. Power Electron.*, vol. 25, no. 10, pp. 2573–2587, Oct. 2010.

[25] Y. Feng, X. Yu, and F. Han, "High-order terminal sliding-mode observer for parameter estimation of a permanent-magnet synchronous motor," *IEEE Trans. Ind. Electron.*, vol. 60, no. 10, pp. 4272–4280, Oct. 2013.

[26] X. Zhang, L. Sun, K. Zhao, and L. Sun, "Nonlinear speed control for PMSM system using sliding-mode control and disturbance compensation techniques," *IEEE Trans. Power Electron.*, vol. 28, no. 3, pp. 1358–1365, Mar. 2013.

[27] W. Gao, Y. Wang, and A. Homaifa, "Discrete-time variable structure control systems," *IEEE Trans. Ind. Electron.*, vol. 42, no. 2, pp. 117–122, Apr. 1995.

[28] W. Gao and J. C. Hung, "Variable structure control of non-linear systems: A new approach," *IEEE Trans. Ind. Electron.*, vol. 40, no. 1, pp. 45–55, Feb. 1993.

[29] J. Pan, W. Li, and H. Zhang, "Control algorithms of magnetic suspension systems based on the improved double exponential reaching law of sliding mode control," *Int. J. Control, Autom. Syst.*, vol. 16, no. 6, pp. 2878–2887, Dec. 2018.

[30] C. J. Fallaha, M. Saad, H. Y. Kanaan, and K. Al-Haddad, "Sliding-mode robot control with exponential reaching law," *IEEE Trans. Ind. Electron.*, vol. 58, no. 2, pp. 600–610, Feb. 2011.

[31] S. M. Mozayan, M. Saad, H. Vahedi, H. Fortin-Blanchette, and M. Soltani, "Sliding mode control of PMSG wind turbine based on enhanced exponential reaching law," *IEEE Trans. Ind. Electron.*, vol. 63, no. 10, pp. 6148–6159, Oct. 2016.

[32] Y. Liu, Z. Wang, L. Xiong, J. Wang, X. Jiang, G. Bai, R. Li, and S. Liu, "DFIG wind turbine sliding mode control with exponential reaching law under variable wind speed," *Int. J. Electr. Power Energy Syst.*, vol. 96, pp. 253–260, Mar. 2018.

[33] B. Brahmi, M. H. Laraki, A. Brahmi, M. Saad, and M. H. Rahman, "Improvement of sliding mode controller by using a new adaptive reaching law: Theory and experiment," *ISA Trans.*, vol. 97, pp. 261–268, Feb. 2020.

[34] D. K. B. and S. Thomas, "Power rate exponential reaching law for enhanced performance of sliding mode control," *Int. J. Control, Autom. Syst.*, vol. 15, no. 6, pp. 2636–2645, Dec. 2017.

[35] G. Rohith, "Fractional power rate reaching law for augmented sliding mode performance," *J. Franklin Inst.*, vol. 358, no. 1, pp. 856–876, Jan. 2021.

[36] S. K. Kommuri, S. B. Lee, and K. C. Veluvolu, "Robust sensors-fault-tolerance with sliding mode estimation and control for PMSM drives," *IEEE/ASME Trans. Mechatronics*, vol. 23, no. 1, pp. 17–28, Feb. 2018.

[37] A. T. Vo, T. N. Truong, and H.-J. Kang, "A novel tracking control algorithm with finite-time disturbance observer for a class of second-order nonlinear systems and its applications," *IEEE Access*, vol. 9, pp. 31373–31389, 2021, doi: 10.1109/ACCESS.2021.3060381.

[38] U. P. Ventura and L. Fridman, "Chattering measurement in SMC and HOSMC," in *Proc. 14th Int. Workshop Variable Struct. Syst. (VSS)*, Jun. 2016, pp. 108–113, doi: 10.1109/VSS.2016.7506900.

[39] J. Dong and J. Zhang, "Higher order sliding mode control for a class of MIMO systems," in *Advanced Materials Research*, vol. 834. Trans Tech Publications Ltd, 2014, pp. 1105–1109.

[40] V. Utkin, A. Poznyak, Y. Orlov, and A. Polyakov, "Conventional and high order sliding mode control," *J. Franklin Inst.*, 2020, doi: 10.1016/j.jfranklin.2020.06.018.

FAHEEM HAROON received the B.Eng. and M.S. degrees in electrical engineering from Bahria University, Islamabad, Pakistan, in 2009 and 2014, respectively. He is currently pursuing the Ph.D. degree in electrical engineering with the Department of Electrical Engineering, Bahria School of Engineering & Applied Sciences Islamabad Campus (BSEAS-IC), Pakistan. His current research interest includes control of voltage source converters for power system applications.

MUHAMMAD AAMIR received the B.Eng. degree (Hons.) in electrical engineering from the University of Engineering and Technology (UET), Peshawar, Pakistan, the master's degree from Hanyang University, South Korea, and the Ph.D. degree from the Power Electronics and Renewable Energy Research Laboratory (PEARL), Department of Electrical Engineering, University of Malaya, Kuala Lumpur, Malaysia. In 2017, he joined Bahria University, as an Assistant Professor. He is currently working as an Assistant Professor with the Pak-Austria Fachhochschule: Institute of Applied Sciences and Technology, Haripur, Pakistan. His research interests include uninterruptible power supplies (UPS), power conversion, and control of power converters.

ASAD WAQAR received the degree in electrical engineering from the UET Taxila, in 2002, the master's degree in electrical power engineering from RWTH Aachen, Germany, in 2011, and the Ph.D. degree in electrical engineering from the Huazhong University of Science and Technology, China, in 2016. He worked for different industries for several years. He is currently working as a Professor with the Department of Electrical Engineering, Bahria School of Engineering & Applied Sciences Islamabad Campus (BSEAS-IC), Pakistan. He has successfully supervised more than 30 master's thesis students. He is also supervising three Ph.D. students at Bahria University as well. He has published research articles in many reputed international journals. His research interests include smart grids, microgrid operation and control, power quality, power electronics, network reinforcement planning, demand side management, and big data analysis in power systems. He serves as an Active Reviewer for *Applied Energy*, *International Transactions on Electrical Energy Systems*, IEEE Access, *Renewable and Sustainable Energy Reviews*, and *International Journal for Engineering Science and Technology*.